Structural Basis for Different Inhibitory Specificities of Human Cystatins C and D[†]

Anders Hall,[‡,§] Irena Ekiel,[||] Robert W. Mason,[⊥] Franciszek Kasprzykowski,[#] Anders Grubb,[‡] and Magnus Abrahamson*[,‡]

Department of Clinical Chemistry, Institute of Laboratory Medicine, University of Lund, University Hospital, S-221 85 Lund, Sweden, Biomolecular NMR Laboratory, Pharmaceutical Biotechnology Sector, Biotechnology Research Institute, National Research Council of Canada and Montreal Joint Centre for Structural Biology, 6100 Royalmount Avenue, Montréal, Quebec H4P 2R2, Canada, Division of Developmental Biology, Nemours Research Programs, P.O. Box 269, Wilmington, Delaware 19899, and Department of Chemistry, University of Gdansk, Sobieskiego 18, 80-952 Gdansk, Poland

Received May 21, 1997; Revised Manuscript Received December 16, 1997

ABSTRACT: Human cystatins C and D share almost identical primary structures of two out of the three segments proposed to be of importance for enzyme interactions but have markedly different profiles for inhibition of the target cysteine peptidases, cathepsins B, H, L, and S. To investigate if the N-terminal binding regions of the inhibitors are responsible for the different inhibition profiles, and thereby confer biological selectivity, two hybrid cystatins were produced in *Escherichia coli* expression systems. In one hybrid, the N-terminal segment of cystatin C was placed on the framework of cystatin D, and the second was engineered with the N-terminal segment of cystatin D on the cystatin C scaffold. Truncated cystatin C and D variants, devoid of their N-terminal segments, were obtained by incubation with glycyl endopeptidase and isolated, in a second approach to assess the importance of the N-terminal binding regions for cystatin function and specificity. The affinities of the four cystatin variants for cathepsins B, H, L, and S were measured. By comparison with corresponding results for wild-type cystatins C and D, it was concluded (1) that both the N-terminal and framework part of the molecules significantly contribute to the observed differences in inhibitory activities of cystatins C and D and (2) that the N-terminal segment of cystatin C increases the inhibitory activity of cystatin D against cathepsin S and cathepsin L but results in decreased activity against cathepsin H. These differences in specificity were explained by the residues interacting with the S_2 subsite of peptidases (Val- and Ala-10 in cystatin C and D, respectively). Also, removal of the N-terminal segment results in total loss of enzyme affinity for cystatin D but not for cystatin C. Therefore, structural differences in the framework parts, as well as in the N-terminal segments, are critical for both inhibitory specificity and potency. Homology modeling was used to identify residues likely responsible for the generally reduced inhibitory potency of cystatin D.

Human cystatins C and D are secretory inhibitors of cysteine peptidases and members of family 2 of the cystatin superfamily. These cystatins may therefore participate both in the extracellular regulation of endogenous cysteine peptidases, such as cathepsins B, H, L, and S, and in the protection against exogenous enzymes released, e.g., at sites of microbial infections (*1*). Whereas cystatin C has a widespread distribution and is ubiquitous in human tissues and body fluids, cystatin D has a more restricted presence and has so far only been found in saliva and tears (*2*−*4*). Cystatin D appears in two allelic variants with either Cys or Arg as residue 26,[1] as a result of a genetic polymorphism, but without any differences in function, stability, or tissue distribution (*6*). In total, there are six secreted human low-molecular-weight inhibitors of the cystatin superfamily known to date (cystatins C, D, E, S, SN, and SA) (*7*), but little is known about the structural basis for their target enzyme specificity and their actual biological function.

The polypeptide chains of family 2 cystatins have been implicated to contain three segments directly involved in the inhibition of cysteine peptidases (*8*) (Figure 1). The wedge-shaped binding region includes two loop-forming segments that have been conserved during the evolution of family 2 cystatins and correspond to the human cystatin C segments Gln-55−Gly-59 and Pro-105−Trp-106. The third interacting segment is the N-terminal segment, ending with the equally conserved Gly-11 residue. In cystatin C, this segment acts as a discrete binding region and contributes to target enzyme affinity independently of contributions from the wedge-shaped binding region. A systematic exchange of Gly-11 for amino acids with larger side chains (*10*) has demonstrated

[†] This work was supported by grants from the Magn. Bergvall, A. Österlund, A. Påhlsson, and G. and J. Kock Foundations, the Medical Faculty of the University of Lund, the Swedish Medical Research Council (Project Nos. 09915 and 05196), the Canadian National Research Council (No. 39985), the National Science Foundation (Grant MCB-9496260), and the Polish Scientific Research Committee (Grant KBN-156/T09/95/08).

* To whom correspondence should be addressed.

[‡] University of Lund.

[§] Present address: Astra Draco AB, Box 34, S-223 62 Lund, Sweden.

[||] National Research Council of Canada and Montreal Joint Centre for Structural Biology.

[⊥] Nemours Research Programs.

[#] University of Gdansk.

[1] Throughout this paper, cystatin residues are numbered after the wild-type cystatin C sequence (*5*).

S0006-2960(97)01197-5 CCC: $15.00
Published on Web 03/05/1998

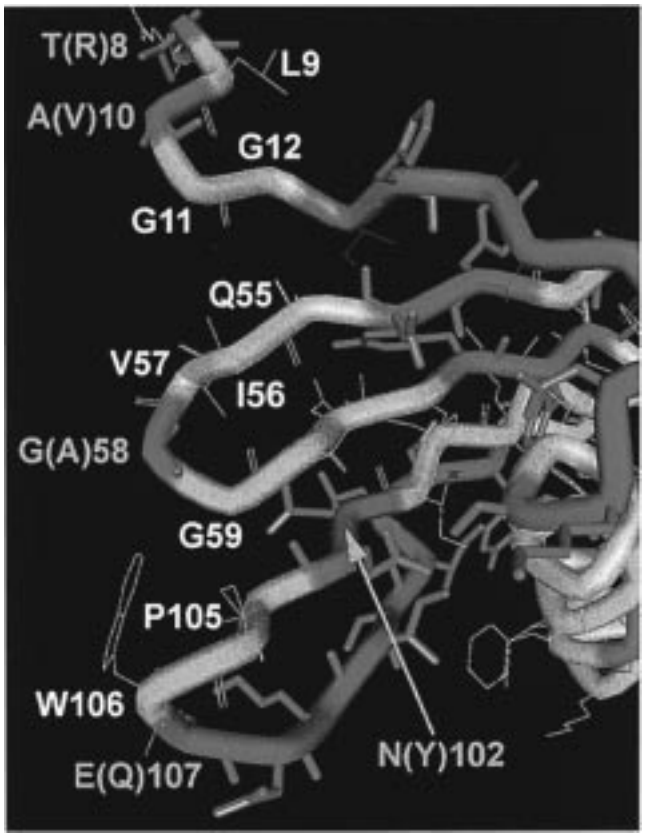

FIGURE 1: Homolgy model of cystatin D. A homolgy model of cystatin D was built on the basis of the X-ray crystal structure of chicken cystatin (*8*) and NMR data for cystatin C (*9*) (see Experimental Procedures). The enzyme-interacting side of the molecule is shown, with the N-terminal cystatin segment and the two loops directly involved in interactions with target enzymes facing left. Residues identical in the cystatin C and D sequences are marked in gray. For positions where residues differ (red), the cystatin D residues are shown in the one-letter code, with the substitutions in cystatin C within parentheses. The numbering refers to the cystatin C sequence (*5*).

that this residue functions as a hinge between the, according to NMR studies, flexible N-terminal segment (*9*) and the rest of the molecule. Gly-11 thereby allows the N-terminal segment to adopt a conformation that is optimal for target enzyme interactions (*10, 11*). The single 120 and 122 residue long polypeptide chains of cystatins C (*5*) and D (*12*), respectively, display 55% amino acid identity. Despite the general sequence homology and conservation of other cystatin characteristics, including the four Cys residues that have been shown to form two disulfide bridges in cystatin C (*13*), cystatins C and D show distinct differences in their affinity profiles for cysteine peptidases. Cystatin C forms tight reversible complexes, with dissociation equilibrium constants in the subnanomolar area, with virtually all cysteine peptidases of the papain superfamily (reviewed in ref 1). Cystatin D, on the other hand, does not inhibit cathepsin B, is a much poorer inhibitor of papain and cathepsin L, but forms tighter complexes with cathepsin S and H (*6*).

Individual amino acids in the N-terminal inhibitor segment contribute significantly to the specificity of cathepsin B, H, L, and S inhibition by cystatin C. However, the total contribution of the N-terminal binding region compared to that of the wedge-shaped binding region varies depending on the target enzyme, which demonstrates that also the wedge-shaped region is important for the normal inhibition profile of cystatin C (*14*). Corresponding data for cystatin D are lacking. The objective of the present investigation was to elucidate the contribution of the N-terminal segments of cystatin C and D to their different specificities for the target enzymes, cathepsins B, H, L, and S. We have used a recombinant DNA approach to exchange the N-terminal segments of the two proteins for each other and compared the inhibitory properties of the two hybrid cystatins with those of cystatin C and D variants lacking the N-terminal segments as well as with those of the wild-type proteins. In addition, peptidyl diazomethyl ketones modeled after the N-terminal segments of cystatins C and D were studied to further assess the inhibitory potential of the N-terminal segments for enzyme interaction.

EXPERIMENTAL PROCEDURES

Materials. Oligonucleotides were synthesized on an Applied Biosystems 392A synthesizer using phosphoramidites and other chemicals from Applied Biosystems (Foster City, CA). Biotin was added to the 5′-end of oligonucleotides to be used for direct sequencing of PCR[2] products, directly at synthesis by use of Biotin-ON Phosphoramidite (Clontech, Palo Alto, CA). Restriction endonucleases and DNA modifying enzymes were from Life Technologies (Gaithersburg, MD). Streptavidin-coated paramagnetic beads ("Dynabeads") were from Dynal AS, Oslo, Norway. The enzyme substrates Cbz-Phe-Arg-NHMec, H-Arg-NHMec, and Bz-Arg-pNA were obtained from Bachem Feinchemikalien (Bubendorf, Switzerland). L-3-Carboxy-2,3-(*trans*-epoxypropionyl)leucylamido-(4-guanidino)butane (E-64) was from Sigma Chemical Co. (St. Louis, MO). Human cathepsins B (EC 3.4.22.1), L (EC 3.4.22.15), and H (EC 3.4.22.16) were from Calbiochem (La Jolla, CA). Bovine cathepsin S (EC 3.4.22.27) was prepared as described previously (*15*). Glycyl endopepidase (EC 3.4.22.25) was a gift from Dr. David Buttle, University of Sheffield, U.K. All standard chemicals used were of analytical grade and were obtained from Sigma.

Escherichia coli Expression. Recombinant wild-type human cystatin C and the natural Arg-26 variant of human cystatin D were produced in *E. coli*, using the expression plasmids pHD313 and pCysD-Arg, respectively, as earlier described (*6, 16*). These two constructs will in the following be referred to as pCysC and pCysD, respectively. Both expression plasmids contain cDNA inserts for the mature cystatins fused in frame after a segment encoding the *E. coli* outer membrane protein A (OmpA) signal peptide. The temperature regulated phage λ cI repressor and P_R promoter serve as controlling elements, resulting in high-level expression and periplasmic space transport of the recombinant cystatins. pCysC, pCysD, and the modified expression plasmids described below were introduced in *E. coli* MC1061. Subclones of bacteria containing expression plasmids were selected by ampicillin resistance and grown overnight, and plasmid DNA was isolated from the cultures by a standard alkaline lysis procedure (*17*).

Polymerase Chain Reaction. PCR amplifications were performed in a Perkin-Elmer−Cetus TC-1 thermocycler

[2] Abbreviations: PCR, polymerase chain reaction; Cbz, carboxybenzoyl; NHMec, 7-(4-methyl)coumarylamide.

Table 1: Oligonucleotides Used for Recombinant DNA Work[a]

oligo	use for	template/strand	sequence
289	*Bam*HI site deletion	pCysD/−	5′-CAGGTCGACTCTAGAG*A*ATCCC-3′
290	*Bam*HI site introduction	pCysD/−	5′-GGTCTGTGGCAT**GGATCC**CACC-3′
291	*Bam*HI site introduction	pCysD/+	5′-GGACCTTGGCAGGTG**GGATCC**A-3′
292	N-terminal fragment with *Nco*I site	pCysD/−	5′-*GA**CCATGG**GG*CCACCTGCCAAGGTC-3′
293	N-terminal fragment with *Bam*HI site	pCysC/−	5′-*GG**GGATCC***CACCAACCAGACGCGGC-3′
206	PCR, sequencing	vector/+	5′-GTTTCGCCTGTCTGTTTTGC-3′
220	PCR, sequencing	vector/−	5′-CGACGTTGTAAAACGACGGC-3′
288	sequencing	pCysD/−	5′-CTTTAGATCCGGCCAAGCTG-3′
011	sequencing	pCysC/−	5′-CCAAGACCCAGCCCAACTTG-3′
078	sequencing	pCysC/−	5′-GTATTCCCACCCCTGGACTG-3′

[a] Nucleotide differences between the PCR primers and the corresponding target sequences in the expression vectors for cystatin C (pCysC) or cystatin D (pCysD) are underlined. Restriction endonuclease recognition sites are indicated by bold type.

using DNA polymerase and other reagents from the Ampli-Taq kit (Perkin-Elmer−Cetus, Norwalk, CT), and if not stated otherwise primers were at 0.6 μM concentration and 0.6 ng of uncleaved plasmid DNA as template in a 100 μL reaction volume. The PCR cycle (1 min at 94 °C, 1 min at 60 °C, 1 min at 72 °C) was repeated 25−30 times. The sequences of all PCR primers used are listed in Table 1. PCR products were purified by phenol/chloroform extractions and ethanol precipitation.

Production of the Hybrid Cystatin DOC. For construction of an expression vector for production of a hybrid cystatin composed of the N-terminal cystatin D segment fused with the cystatin C framework molecule, in the following called cystatin DOC (cystatin ***D*** N-terminal segment ***o***n cystatin ***C***), two unique recognition sites in pCysC for the restriction endonucleases *Cla*I and *Nco*I were used. The *Cla*I-*Nco*I fragment, which includes the coding sequence for the OmpA signal peptide as well as cystatin C residues 1−14, was excised. Plasmid pCysD shares the upstream vector site for *Cla*I but lacks a corresponding downstream *Nco*I site in the cDNA insert. By a PCR with pCysD as template, the (+) strand primer 206, corresponding to a vector segment and encompassing the *Cla*I site (*14*), was used together with the (−) strand primer 292, corresponding to the cystatin D sequence for residues 8−11 and with a 5′-tail containing the coding sequence for cystatin C residues 12−14 and including the unique *Nco*I site, to amplify a 182 base pair fragment. The amplification product was purified, cleaved with *Cla*I and *Nco*I, and then ligated into the *Cla*I−*Nco*I opened and dephosporylated pCysC to create plasmid pCysDOC (Figure 2).

Production of the Hybrid Cystatin COD. To engineer an expression vector for production of a second hybrid cystatin, composed of the N-terminal cystatin C segment fused with the cystatin D framework molecule, in the following called cystatin COD (cystatin ***C*** N-terminal segment ***o***n cystatin ***D***), no unique cleavage sites in the cystatin D insert of pCysD were present to allow direct exchange of a fragment encoding the N-terminal segment for that of cystatin C. In the pCysD construct there is one unique site for *Bam*HI downstream from the cDNA insert. By use of site-directed mutagenesis this *Bam*HI site was knocked out and a new *Bam*HI site was introduced by a single base substitution at a position corresponding to amino acid residue 13 (Figure 2). This was achieved by a first PCR in which primers 206 and 290 were used to create the new *Bam*HI site. A second PCR utilized primer 291 to partly overlap primer 290 and primer 289 to knock out the old vector site for *Bam*HI. The two

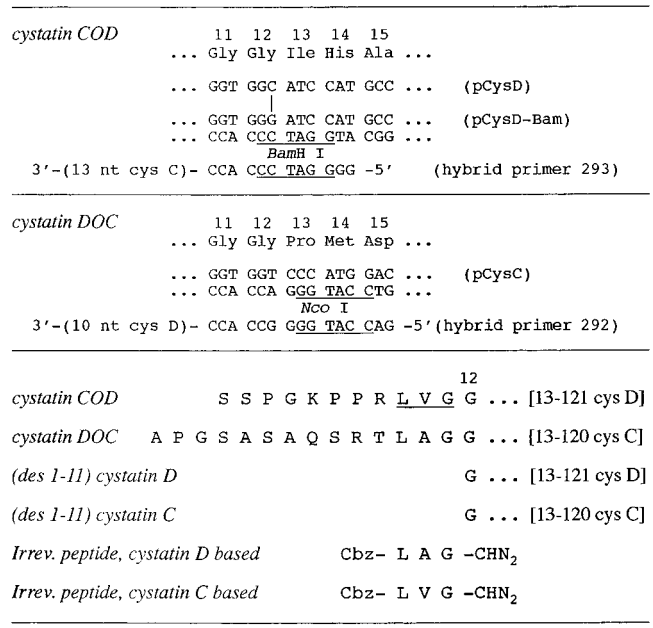

FIGURE 2: Construction and primary structure of cystatin C/D hybrids. Top panel: The hybrid cystatin COD was constructed by removal of a *Cla*I−*Bam*HI fragment encoding the cystatin D N-terminal segment from expression plasmid pCysD-Bam, the latter being a variant of pCysD (see Experimental Procedures). A *Cla*I−*Bam*HI fragment encoding the cystatin C N-terminal segment was achieved by PCR with a vector primer 206 and the indicated hybrid primer 293, using pCysC as template. The cystatin C N-terminal encoding segment was then ligated to the *Cla*I/*Bam*HI opened pCysD-Bam. Middle panel: The hybrid cystatin DOC was similarly constructed by removal of a *Cla*I−*Nco*I fragment encoding the cystatin C N-terminal segment from expression plasmid pCysC, followed by ligation of a *Cla*I−*Nco*I fragment encoding the cystatin D N-terminal segment which had been generated by PCR with a vector primer 206 and the indicated hybrid primer 292, using pCysD as template. Bottom panel: The N-terminal amino acid sequences of the hybrid cystatins COD and DOC and glycyl endopeptidase truncated cystatins C and D are shown in the standard one-letter code. The synthetic peptidyl diazomethyl ketones used, with peptidyl parts modeled after the proposed $P_3-P_2-P_1$ residues of the N-terminal cystatin C or D segments are aligned below. The N-terminal cystatin C residues shown to be important for target enzyme interactions (*10*, *14*) are underlined in the sequence of cystatin COD.

PCR products were mixed, and three cycles of annealing and elongation were accomplished before primers 206 and 289 were added to amplify the full-length cystatin sequence. This final PCR product, corresponding to the entire OmpA-cystatin D cDNA insert of pCysD, was cleaved with *Cla*I and at a second unique downstream vector site, for *Xba*I (*4*). The cleaved PCR product was ligated into pCysD previously

opened with *Cla*I and *Xba*I and dephosphorylated to create the modified plasmid pCysD-Bam. By a PCR with pCysC as template, the (+) strand vector primer 206 was used together with the (−) strand primer 293 (corresponding to the cystatin C sequence for residues 7−11 and with a 5′-tail containing the coding sequence for cystatin D residues 12−13, as well as including the novel *Bam*HI site of pCysD-Bam; Figure 2) to amplify a 169 base pair fragment. This amplification product was purified, cleaved with *Cla*I and *Bam*HI, and then ligated into the *Cla*I−*Bam*HI opened and dephosphorylated pCysD-Bam to create plasmid pCysCOD.

Verification of DNA Constructs. Expression plasmid constructs were verified by DNA sequencing of the plasmid isolated from bacterial subclones obtained after transformation and selection. For pCysDOC the entire coding sequence was amplified by PCR using a biotinylated upstream primer 206(b) and a nonbiotinylated downstream primer 220. Primer concentrations were 1.2 μM, but otherwise the PCR conditions were the same as described above. The coding strand of the PCR product was separated from the noncoding strand after binding to streptavidin-coated beads, as described by the bead supplier (Dynal). The coding strand on the streptavidin beads was used as template in dideoxy sequencing using reagents in the Sequenase version 2.0 kit (United States Biochemical, Cleveland, OH) and oligonucleotide 011 or 078 (Table 1) as primer. The noncoding strand served as template in sequencing reactions with nonbiotinylated oligonucleotide 206 as primer. The sequencing of pCysCOD followed the same procedure, but primer 288 was used instead of primer 220.

Production and Isolation of the Hybrid Cystatins DOC and COD. Growth conditions for cultures of bacterial subclones containing the two expression plamids, as well as conditions for induction of expression of the recombinant genes, were exactly as previously described (*10*). From 0.5 L cultures of each, a 20 mL periplasmic extract was obtained by cold osmotic shock (*18*). Isolation of the recombinant hybrid cystatins was achieved by affinity chromatography on immobilized polyclonal rabbit antisera against recombinant cystatin C or D, using 50 mM Tris containing 6 M GuHCl as elution buffer, followed by gel chromatography on a Pharmacia FPLC Superdex 75 column in 0.1 M ammonium bicarbonate buffer, pH 8.0. The salt-free solutions of the isolated hybrid cystatins were concentrated by ultrafiltration (Centricon 3; Amicon Corp., Danvers, MA) to approximately 0.2 mg/mL when necessary and were stored frozen at −20 °C until used.

Generation of Cystatin C and D Variants with Truncated N-Terminal Segments. Samples of 500 μL of cystatin C and D solutions at 0.5 mg/mL in 0.1 M ammonium bicarbonate buffer, pH 8.0, were mixed with 20 μL of a 1 mg/mL solution of glycyl endopeptidase in 50 mM phosphate buffer, pH 6.5. The mixtures were incubated at 37 °C for 2 h, whereafter electrophoresis revealed that the native cystatins in both mixtures had been converted to forms with altered electrophoretic mobilities. The main products from the incubation mixtures were purified using gel filtration on a Pharmacia FPLC Superdex 75 column in 0.1 M ammonium bicarbonate buffer, pH 8.0.

Protein Characterization. The isolated recombinant hybrid cystatins and the N-terminally truncated variants were characterized by SDS−polyacrylamide electrophoresis after reduction in 16.5% gels with the buffer system described by Schägger and von Jagow (*19*) and by automated N-terminal sequencing (*20*) using equipment and detailed procedures described earlier (*10*). The temperature stability of the cystatin variants (in 0.1 M ammonium bicarbonate buffer, pH 8.0) was studied by 30 min incubations of samples at various temperatures, followed by centrifugation and immunoassay of remaining soluble protein, as detailed earlier (*14*).

Peptidyl Derivatives. The amino acid derivatives used in the syntheses described below were obtained from Nova-Biochem. The melting points given are uncorrected. Optical rotations were measured on a Perkin-Elmer 141 polarimeter. Samples for analytical purposes were dried over P_2O_5 in vacuo for 24 h. The structures of synthesized products were confirmed by NMR (Varian XL-200) and IR (Specord 71 IR spectrometer) spectra. The structures of the peptidyl diazomethyl ketones were additionally confirmed by FAB-MS. Thin-layer chromatography was carried out using silica gel plates (Merck) and as eluents the following solvent systems: (A) benzene−acetone−acetic acid (2:1:0.05); (B) benzene−acteone (2:1).

The synthesis of Cbz-Leu-Val-Gly diazomethyl ketone (Cbz-Leu-Val-Gly-CHN_2), with the peptidyl portion modeled after the cystatin C N-terminal segment, has been described earlier (*21*). Cbz-Leu-Ala-Gly-CHN_2, with the peptidyl portion modeled after the cystatin D N-terminal segment, was produced using a similar protocol: HCl H-Ala-Gly-OMe (0.62 g, 3.13 mmol) was coupled with Cbz-Leu-OH (1 g, 3.75 mmol) in tetrahydrofuran using the DCCI/HOBt activation method and triethylamine (0.44 mL, 3.13 mmol) to achieve Cbz-Leu-Ala-Gly-OMe. The product was recrystallized from toulene−petroleum ether (bp = 35−55 °C) [yield, 1.2 g (93%), mp = 144−146 °C, $[\alpha]^{20}_D = -45.4°$ ($c = 1$, methanol), $R_f = 0.55$ (solvent system A)]. The Cbz-Leu-Ala-Gly-OMe (1.1 g, 2.7 mmol) was dissolved in 10 mL of methanol, 1 N NaOH/H_2O (2.7 mL) was added to the solution at 0 °C, hydrolysis was performed during 2 h, and the mixture was then acidified to pH 2 with 2 N HCl. The precipitated product was filtered off, dried, and recrystallized from dioxane−diethyl ether [yield, 0.76 g (71.5%), mp = 130−132 °C, $[\alpha]^{20}_D = -43.3°$ ($c = 1$, methanol), $R_f = 0.17$ (solvent system A)]. The resulting Cbz-Leu-Ala-Gly-OH was used to synthesize Cbz-Leu-Ala-Gly-CHN_2 (in 1.4 mmol scale) in accordance with the procedure used for Cbz-Leu-Val-Gly-CHN_2 (*19*). The crude product was purified by gel filtration using a Sephadex LH-20 column (Pharmacia) and methanol as eluent [yield, 0.18 g (31%), mp = 142−145 °C (dec), $[\alpha]^{20}_D = -21.9°$ ($c = 1$, methanol), $R_f = 0.26$ (solvent system B)].

The peptidyl diazomethyl ketones were dissolved in dimethyl sulfoxide, and the solutions were then diluted to 1% (v/v) dimethyl sulfoxide using 0.01% (v/v) Brij-35.

Enzyme Inhibition Assays. The methods used for determination of equilibrium constants for dissociation (K_i) of complexes between cystatins and cysteine peptidases, and for purification of papain for use in active site titrations, have been described in detail earlier (*1*). In brief, continuous rate assays with fluorogenic substrates were employed in 100 mM sodium-phosphate buffer, pH 6.0, containing 1 mM dithiothreitol and 2 mM EDTA. The substrates used were Cbz-Phe-Arg-NHMec (10 μM) for cathepsins B, L, and S and

H-Arg-NHMec (10 μM) for cathepsin H. For the protein variants, steady-state velocities before and after addition of inhibitor were measured, and apparent K_i values were calculated according to the equation described by Henderson (*22*). For the irreversible peptidyl inhibitors, pseudo-first-order rate constants were measured and used to calculate apparent second-order rate constants by dividing with assay inhibitor concentrations. The apparent equilibrium and rate constants were corrected for substrate competition using K_m values of 150 and 7 μM for cathepsins B and L, respectively (*23*), 15 μM for cathepsin S, and 40 μM for cathepsin H (*15*).

Homology Modeling for Cystatin D. A computer model of cystatin D was constructed on the basis of previously published sequence alignments (*12*). For this purpose, chicken cystatin coordinates (1CEW; *8*) served as a starting point. Corresponding amino acids were mutated using the program Sybyl 6.2 (Tripos). Unfavorable interactions between residues were adjusted manually, after which energy was minimized using Kollman force field parameters (*24, 25*) implemented in the Sybyl software package.

RESULTS

Production and Characterization of Cystatin C and D Variants with Modified N-Terminal Segments. To allow studies of the importance of the cystatin C and D N-terminal segments for target enzyme specificity at inhibition, two recombinant cystatin hybrids were created. The hybrid called cystatin DOC was designed as a cystatin C molecule with the N-terminal segment replaced by that of cystatin D and cystatin COD as a cystatin D molecule with the N-terminal segment exchanged for that of cystatin C, as described under Experimental Procedures. In both hybrids, the resulting fusion point between cystatin C and D polypeptide chain segments was the evolutionary conserved Gly-11 residue (Figure 2). The two hybrid variants were isolated by affinity chromatography from the periplasmic fraction of bacterial cultures after expression had been induced in the secretory *E. coli* expression system used. This resulted in preparations of the two variants with a purity of at least 95%, as assessed by polyacrylamide gel electrophoresis (Figure 3).

In a second approach to study the importance of their N-terminal segments, cystatins C and D were incubated with glycyl endopeptidase, an enzyme previously shown to hydrolyze a single N-terminal segment bond in human cystatin C (*26, 27*). The incubations resulted in cleavage of a single bond at Gly-11−Gly-12 in both inhibitors (see below). The thereby modified cystatins, designated (des 1−11) cystatins C and D, were isolated by gel filtration, as described under Experimental Procedures.

For all four cystatin variants, the SDS−PAGE estimated M_r was slightly higher than the M_r calculated from their sequences but comparable to that obtained by the same SDS−PAGE system for the native proteins (*6, 16*). The two cystatin hybrids and wild-type recombinant cystatins C and D all eluted on a calibrated Superdex 75 column at a position corresponding to an M_r of 12 400 and the two truncated cystatin variants to an M_r corresponding to the loss of 11−12 amino acids. The two cystatin hybrids and the glycyl endopeptidase truncated cystatin D were subjected to automated Edman degradation (15, 15, and 5 steps, respectively).

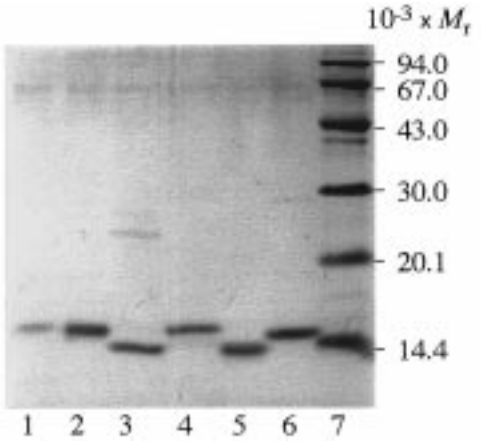

FIGURE 3: SDS−PAGE of cystatin variants. The protein variants were subjected to electrophoresis in a 16.5% polyacrylamide gel. Lanes: 1, cystatin COD; 2, cystatin DOC; 3, (des 1−11) cystatin D; 4, cystatin D; 5, (des 1−11) cystatin C; 6, cystatin C. The sample in lane 3 was electrophoresed prior to the gel filtration used to remove the glycyl endopeptidase added to achieve N-terminal truncation; all others are the final preparations used for inhibition studies. The size markers shown in the lane to the right are phosphorylase *b* (M_r 94 000), bovine serum albumin (M_r 67 000), ovalbumin (M_r 43 000), carbonic anhydrase (M_r 30 000), soybean trypsin inhibitor (M_r 20 100) and α-lactalbumin (M_r 14 400).

The released amino acid phenylthiohydantoin derivatives verified in every position the expected N-terminal sequences (data not shown). The combined results of the physiochemical characterization of the cystatin variants, along with DNA sequencing of the coding regions of the expression vectors present in the same bacterial cultures as were used for expression of the two cystatin hybrids, fully supported that the variants produced were those intended.

A three-dimensional model of cystatin D was constructed using homology modeling based on the chicken cystatin structure (Figure 1). This model was inspected for consistency and for conservation of secondary and tertiary structure. Amino acids in the region homologous to that forming an α-helix in chicken cystatin can be arranged in a helix with similar amphiphilic character in all the human family 2 cystatins. In particular, there is a clear pattern of hydrophobic amino acids Val/Leu-Xaa-Xaa-Ala-Leu-Xaa-Phe-Ala-Ile/Val/Met (residues 23−31), which form an interface between the helix and a five-stranded β-sheet of the family 2 cystatins. The highly conserved amino acids Tyr-34 and Asn-35 at the C-end of the helix also participate in interactions with the β-sheet. Additionally, the β-sheet provides numerous amino acids contributing to the hydrophobic core of cystatins (*8*). This is reflected by a pattern of alternating hydrophobic and predominantly hydrophilic amino acids, most clearly seen on the second and the third strand of the β-sheet. In chicken cystatin, amino acids Val-46, Val-49, Ala-52, Tyr-62, Leu-64, Val-66, Ile-68, Cys-97, Phe-99, Val-101, Ile-110, and Leu-112 contribute to the hydrophobic core. In all these positions hydrophobic amino acids are also present in cystatin D (as well as in cystatins C, S, SN, and SA). These observations support a close similarity of the arrangement of the β-sheet and the relative orientation of the α-helix to the β-sheet in all family 2 cystatins. This is in striking contrast to the family 1 cystatins (or "stefins"), where a difference in the helix orientation causes significant difference in the pattern of hydrophobic

amino acids in the α-helix region. In the cystatin D sequence there is an insertion of one amino acid compared to the other members of cystatin family 2. Most likely this amino acid causes an extension of the loop between the α-helix and the *β*-sheet, consistent with both local sequence homology and hydrophobic amino acid patterns contributing to the protein core. This loop is on the opposite side to the peptidase-interacting region of the molecule, and since it is located on the surface of the protein, it could easily be extended by one amino acid. It is notable that, although overall sequence homology between cystatin D and other cystatins is 40−55%, the most variable regions comprise the N-terminal segment (up to the N-end of the α-helix) (Figure 1) and the last strand of the *β*-sheet. Therefore, homology in the remaining part of the protein, where intramolecular interactions are most critical for the overall fold, is significantly higher, additionally strengthening our conclusion of a very close topological similarity between cystatin D and chicken cystatin. The model furthermore predicts that the two loops participating in binding to cysteine peptidases (containing residues 55−59 and 105−106) (Figure 1) have similar length and conformation. The N-terminal segment of cystatin D is, like those of cystatin C and chicken cystatin (*9, 28*), expected to be flexible and not to interact directly with the rest of the molecule. Therefore, the hybrid and N-terminally truncated protein variants should retain the three-dimensional cystatin structure.

To verify native folds of the cystatin variants lacking N-terminal segments, these were analyzed in temperature stability assays. In agreement with results from corresponding analyses of wild-type cystatin C and recombinant cystatin C variants with single substitutions in the N-terminal segment or the second hairpin loop (*14*), both wild-type and (des 1−11) cystatin D displayed a high temperature resistance, with temperatures for 50% inactivation after 30 min incubation of 83 and 85 °C, respectively (Figure 4A). The corresponding temperatures for wild-type and (des 1−11) cystatin C were 81 and 74 °C, respectively (Figure 4B). Thus, a drastically decreased temperature resistance as has been observed for the aggregation-prone L68Q cystatin C variant due to loss of the correct cystatin fold (*29, 30*) was not observed. Together with the lack of cleavage beyond the exposed N-terminal Gly-Gly bond upon cystatin C and D incubation with glycyl endopeptidase (demonstrated by the electrophoresis and sequencing results above), this strongly suggested that the N-terminally truncated cystatins retained native cystatin folds.

Enzyme Inhibitory Properties of Cystatin Variants. The equilibrium constants for dissociation (K_i) of wild-type cystatins C and D, of the hybrid cystatins COD and DOC, and of the (des 1−11) variants of cystatins C and D in complexes with cathepsins B, H, L, and S were determined from continuous-rate enzyme assays. The preparations of the protein variants used in the inhibition experiments, as well as the peptidyl diazomethyl ketones described below, were all at least 70% active (calculated from results of titrations of affinity purified papain and quantitative amino acid analysis or weighing of proteins and peptides, respectively).

Of the two wild-type cystatins, cystatin C is the more efficient inhibitor against all enzymes studied. Removal of its N-terminal segment, in (des 1−11) cystatin C, decreases

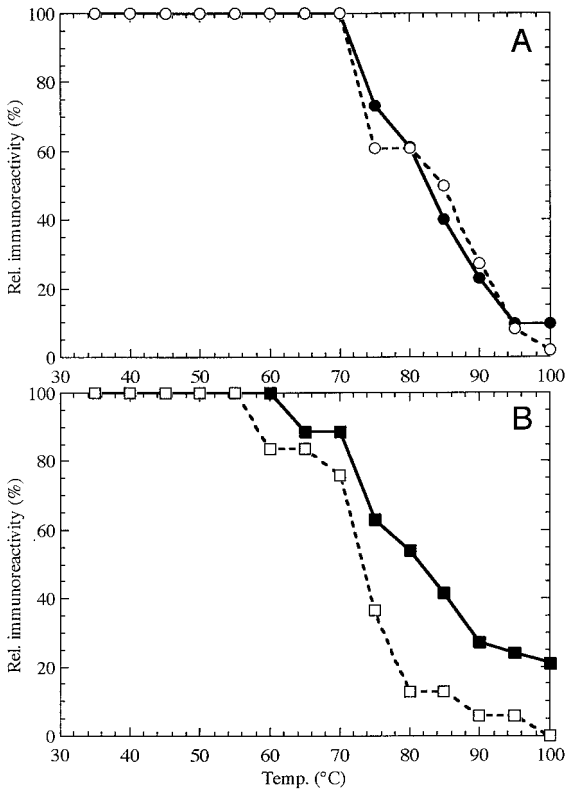

FIGURE 4: Temperature stability of N-terminally truncated cystatins. Samples of isolated wild-type and (des 1−11) cystatins were incubated for 30 min at different temperatures. Remaining cystatin immunoreactivity of sample supernatants following incubation and centrifugation was determined by single radial immunodiffusion and related to the immunoreactivity of a sample kept on ice during the experiment. (A) Full-length (closed circles) and N-terminally truncated (open circles) cystatin D. (B) Full-length (closed squares) and N-terminally truncated (open squares) cystatin C. Corresponding experiments have been reported for a number of cystatin C variants with amino acid substitutions (*14, 29*).

the affinity for all tested enzymes, corresponding to a K_i value change of ≫3 orders of magnitude for cathepsin B, >2 orders of magnitude for cathepsin L and cathepsin S, and 1.5 order of magnitude for cathepsin H. The N-terminal segment of cystatin C thus influences the physiological inhibition and helps in defining the target enzyme inhibition profile for the full-length inhibitor (from the highest affinity to the lowest) as cathepsin L = S > B > H (Figure 5A).

The N-terminal segment of cystatin D results in a similar positive contribution to target enzyme affinity. Removal of the N-terminal segment, in (des 1−11) cystatin D, practically abolishes the affinity of the inhibitor for the tested enzymes (Figure 5B). From these results it follows that the contribution of the cystatin D N-terminal segment to the inhibition of cathepsin L corresponds to a K_i value change of at least 2 orders, cathepsin S with at least 4 orders, and cathepsin H with at least 2 orders of magnitude. The cathepsin B binding potential of the cystatin D N-terminal segment could not be assessed this way, because the full-length inhibitor showed an affinity for this enzyme too low to be measured (K_i > 1 μM). However, the N-terminal segment of cystatin D is less advantageous for cathepsin B inhibition than that of cystatin C, since the hybrid cystatin DOC displays a decreased affinity for cathepsin B corresponding to a K_i value change of 1.5 orders of magnitude compared to wild-type cystatin C. The better cathepsin B binding properties of the N-

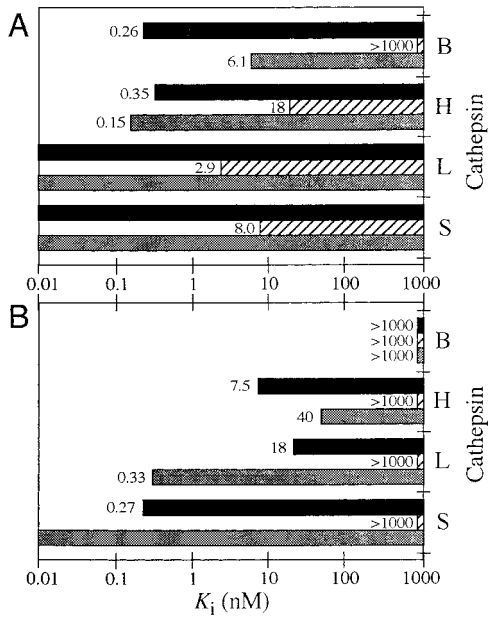

FIGURE 5: Equilibrium constants for dissociation (K_i) of cystatin C/D variant complexes with cathepsins B, L, H, and S. For all interactions, the equilibrium constants were determined from at least five continuous-rate enzyme assays with varying amounts of added cystatin. The values shown by the bars are mean values [all with a variation, (standard deviation)/(mean), < 15%] and were corrected for substrate competition. (A) Investigation of cystatin C based variants: black, full-length wild-type cystatin C; hatched, (des 1−11) cystatin C; gray, cystatin DOC. (B) Cystatin D based variants: black, full-length cystatin D; hatched, (des 1−11) cystatin D; gray, cystatin COD. The full-length bars ending at 0.01 nM on the K_i scale all represent affinities that were too tight to measure ($K_i \ll 0.01$ nM).

terminal segment of cystatin C did not result in sufficiently improved affinity for the hybrid cystatin COD to attain a significant inhibition of cathepsin B.

The N-terminal segment of cystatin C in the hybrid cystatin COD has a positive effect on the affinity of the hybrid cystatin, corresponding to a K_i value change of about 1.5 orders of magnitude for cathepsin L and at least 1 order of magnitude for cathepsin S, compared to wild-type cystatin D. On the other hand, the N-terminal segment of cystatin D is advantageous for inhibition of cathepsin H. This follows from the cathepsin H inhibition results for both the hybrid cystatin DOC, which is more efficient than wild-type cystatin C, and the hybrid cystatin COD, which is less efficient than wild-type cystatin D (Figure 5).

In an additional approach to elucidate the inhibitory potential of the cystatin C and D N-terminal segments, tripeptidyl diazomethyl ketones modeled after cystatins C and D were used (Figure 2). The second-order rate constants, k'_{+2}, for the Cbz-Leu-Val-Gly-CHN_2 (resembling cystatin C) and Cbz-Leu-Ala-Gly-CHN_2 (based on the cystatin D N-terminal sequence) inactivation of the investigated cysteine peptidases were, for cathepsin B, 10 400 and 1980 $M^{-1}s^{-1}$, respectively, for cathepsin L, 35 700 and 930 M^{-1} s^{-1}, for cathepsin S, 53 200 and 1820 M^{-1} s^{-1}, and for cathepsin H in both cases, <100 M^{-1} s^{-1}. The faster cathepsin B, L, and S inactivation by the inhibitor based on the cystatin C N-terminal segment agrees with the results from the hybrid and truncated cystatins.

DISCUSSION

The aim of the present investigation was to find structural explanations to the different specificities of cystatins C and D against the target enzymes cathepsins B, L, H, and S. Wild-type cystatin C inhibits these enzymes in an order of preference (from the highest affinity to the lowest) of cathepsin L = S > B > H whereas cystatin D inhibits in the order S > H > L > B (Figure 5). The secondary structure of human cystatin C, elucidated by NMR spectroscopy (*9*), is almost identical to that of chicken cystatin. The model of cystatin D derived from homology modeling points to close structural similarity between cystatin D and chicken cystatin, including the size of the loops in contact with target peptidases. Most of the amino acids comprising that interface are identical in cystatins C and D (Figure 1). Differences in the sequences forming the interface can be directly responsible for a generally lowered enzyme affinity of cystatin D compared to cystatin C and may at least partly explain the distinct inhibition profile differences of the two cystatins. Additionally, even with overall conformation preserved, the amino acid substitutions may lead to small local conformational differences in the loops, which could affect the activity.

The N-terminal cystatin segment contributes some specificity to the interaction with the target enzymes in the case of cystatin C (*14*). The data presented here suggest that the N-terminal segments of cystatins C and D most likely interact in a generally similar fashion when the inhibitors inhibit cathepsins L, H, and S. This follows from the large negative effect on affinity for these three enzymes upon removal of the entire N-terminal segment of cystatin D, an effect analogous to that seen for similarly truncated cystatin C and in agreement with results for chicken cystatin (*26*, *31*, *32*). However, the (des 1−11) variant of cystatin D is practically devoid of activity against all peptidases, being less potent with a factor corresponding to a K_i value difference of at least 2 orders of magnitude compared to the (des 1−11) variant of cystatin C. The very low activity of the (des 1−11) variant of cystatin D is most likely caused either by the presence of Gly-58 (Figure 1) in the first hairpin loop (the only amino acid different from cystatin C in this region) or by the replacement of Tyr-102 by Asn (Figure 1) since Tyr-102 is highly conserved among cystatins with high inhibitory potency.

The N-terminal sequence of cystatin D is quite different from that of cystatin C and can be responsible for the different inhibition profiles of the cystatins. To investigate this possibility, two hybrid cystatins with exchanged N-terminal segments were created. It is likely that the N-terminal segment of cystatin D is disordered, similarly to what has been found for the N-terminal segments of cystatin C (*9*) and the more distantly related cystatin, stefin A (*33*). Flexible amino acids preceding Gly-12 (Figure 1) should adopt conformationally upon binding to target peptidases, similarly to what was observed in the X-ray structure of a cystatin (stefin) B−papain complex (*34*). Therefore, extensive sequence modifications in the N-terminal segment should be possible without causing structural pertubations in the remaining part of the molecule. The undisturbed thermal stabilities we observed for (des 1−11) cystatins C and D (Figure 4) confirm that this is indeed the case and

moreover show that the cystatin variants investigated are correctly folded. When binding target peptidases, the evolutionary conserved Gly-11 residue would be situated in the P_1 position, and the side chains of Ala-10, Leu-9, and Thr-8 in the N-terminal segment of cystatin D (Val-10, Leu-9, and Arg-8 in cystatin C) would be free to interact with the enzyme S_2, S_3 and S_4 subsites (*8*, *21*). Since the S_3 subsite interacting residue is identical in the two cystatins, the differences in affinity contribution noted should then mainly depend on the proposed S_2 subsite interacting residue, which is Val- and Ala-10 for cystatins C and D, respectively.

Cathepsin B. The so-called occluding loop of cathepsin B does not allow the cystatins to interact with this enzyme as they do with papain (*35*). The inhibition of cathepsin B by cystatin C is dependent on a high association rate constant, facilitated by good initial contact of the N-terminal segment (*36*, *37*). The hybrid cystatin DOC is less efficient than wild-type cystatin C for cathepsin B inhibition, by a factor corresponding to about 1.5 orders of magnitude in K_i value change. This points to a profound importance of an optimal P_2 cystatin residue to interact with a deep S_2 pocket of this enzyme, such as the hydrophobic Val-10 in wild-type cystatin C or a charged Arg-10 as in a cystatin C variant studied in earlier mutagenesis work (*38*), instead of a small Gly-10 residue (*14*) or the Ala-10 present in cystatin D. The approximate 5 times faster inactivation of cathepsin B by Cbz-Leu-Val-Gly-CHN_2 than by Cbz-Leu-Ala-Gly-CHN_2 observed in the present study agrees with this.

Cathepsin H. Our present results clearly indicate that the wedge-shaped binding regions of cystatins C and D interact differently in the inhibition of cathepsin H. Given the pronounced aminopeptidase activity of cathepsin H (*15*), it is not surprising that the mechanism of cystatin inhibition of this enzyme is more complex. Our results for (des 1−11) cystatins C and D show that the N-terminal segments of both inhibitors improve the cystatin affinity for cathepsin H considerably (>100-fold; Figure 5). In the case of cystatin D, the contribution of the N-terminal segment is even a prerequisite for any cathepsin H inhibition at all. Although wild-type cystatin C is a tighter binding cathepsin H inhibitor than cystatin D, its N-terminal segment is less advantageous than that of cystatin D for cathepsin H affinity according to our results. The residue that proposedly interacts with the S_3 subsite, Leu-9, is present also in cystatin D. The better contribution of the cystatin D N-terminal region (reflected by a 2.5-fold higher affinity of cystatin DOC than of wild-type cystatin C and a 5-fold higher affinity of wild-type cystatin D than of cystatin COD) is likely due to a favorable Ala-10 side-chain interaction with a shallow S_2 pocket of cathepsin H, in agreement with a preference for small P_2 residues in endopeptidase substrates for cathepsin H (*15*).

Cathepsin S. The N-terminal segments of cystatins C and D contribute to the inhibition of cathepsin S with an affinity corresponding to >3 orders of magnitude in K_i value change, and the effects of N-terminal segment truncation are similar for both inhibitors. From a comparison of the affinities of cystatin D and cystatin COD, it follows that a Val residue in the P_2 position (cystatin C) instead of an Ala (cystatin D) has a positive effect on cystatin affinity for this enzyme, corresponding to >1 order of magnitude in K_i value change. This is supported by the peptidyl diazomethyl ketone results; Cbz-Leu-Val-Gly-CHN_2 is a 29 times faster cathepsin S inhibitor than Cbz-Leu-Ala-Gly-CHN_2. The Gln-55−Gly-59 segment has been shown to be of high importance for cystatin C inhibition of cathepsin S (*14*). Cystatin D inhibits cathepsin S more efficiently than it does any of the other tested enzymes, and a similar mode of important interaction from this region in cystatin D is thus proposed from our results.

Cathepsin L. The importance of the cystatin P_2 residue for specificity of inhibition is shown by comparison of data for interactions between the cystatin variants and cathepsin L. The hybrid cystatin COD is more efficient than cystatin D in the inhibition of cathepsin L, with an affinity difference corresponding to about 1.5 orders of magnitude in K_i value change, showing that the hydrophobic Val-10 is preferred over Ala-10 for interaction with a deep S_2 pocket of cathepsin L. Since cystatin D is at least a 10 000-fold less efficient inhibitor of cathepsin L than cystatin C, this points to a profound importance also of the wedge-shaped region for cystatin specificity. Substitutions in the first hairpin loop of this region (the Gln-55−Gly-59 segment) have been shown to be of little importance for chicken cystatin inhibition of cathepsin L (*39*) and are likely of smaller importance also for cystatin C inhibition of cathepsin L, since chicken cystatin and human cystatin C have very similar inhibitory activity against all enzymes studied (*32*). It therefore seems unlikely that the only variability between cystatins C and D in this loop, Ala/Gly in position 58 (Ser in chicken cystatin), can be a main factor to explain the different cathepsin L affinities of the inhibitors. The Trp-106 side chain of the second hairpin loop contributes to the cystatin C affinity for cathepsin L with a factor corresponding to at least 3 orders of magnitude in K_i value change (*14*, *37*). From this it can be inferred that the drastically lower cystatin D affinity for this enzyme likely is due to some differences in the interactions of the Trp residues and the second hairpin loops of cystatin C and D with cathepsin L.

Conclusions. Our results for the hybrid cystatin COD indicate that addition of an N-terminal tail, with sequence based on optimal substrates for a given cysteine peptidase, to the cystatin D framework molecule should provide a feasible approach to create enzyme-specific cystatins. This statement is based on the observations that (1) (des 1−11) cystatin D is practically inactive as an inhibitor, (2) placing of the cystatin C N-terminal segment in cystatin COD results in dramatically increased affinity for three (but not the fourth) of the enzymes studied, and (3) addition of the cystatin C N-terminal segment results in a drastic shift in target enzyme specificity (an affinity increase corresponding to 2 orders of magnitude in K_i value change for cathepsins S and L, but a decrease by 5-fold for cathepsin H, compared to wild-type cystatin D).

ACKNOWLEDGMENT

We thank Dr. David Buttle for the generous gift of glycyl endopeptidase and Dr. Traian Sulea for helpful discussions. The expert technical assistance of Mrs. Anne-Cathrine Löfström is gratefully acknowledged.

REFERENCES

1. Abrahamson, M. (1994) *Methods Enzymol. 244*, 685−700.
2. Abrahamson, M., Barrett, A. J., Salvesen, G., and Grubb, A. (1986) *J. Biol. Chem. 261*, 11282−11289.

3. Abrahamson, M., Olafsson, I., Palsdottir, A., Ulvsbäck, M., Lundwall, Å., Jensson, O., and Grubb, A. (1990) *Biochem. J. 268*, 287−294.
4. Freije, J. P., Balbín, M., Abrahamson, M., Velasco, G., Dalbøge, H., Grubb, A., and López-Otín, C. (1993) *J. Biol. Chem. 268*, 15737−15744.
5. Grubb, A., and Löfberg, H. (1982) *Proc. Natl. Acad. Sci. U.S.A. 79*, 3024−3027.
6. Balbin, M., Hall, A., Grubb, A., Mason, R., López-Otín, C., and Abrahamson, M. (1994) *J. Biol. Chem. 269*, 23156−23162.
7. Ni, J., Abrahamson, M., Zhang, M., Alvarez Fernandez, M., Grubb, A., Su, J., Yu, G.-L., Li, Y., Parmelee, D., Xing, L., Coleman, T. A., Gentz, S., Thotakura, R., Nguyen, N., Hesselberg, M., and Gentz, R. (1997) *J. Biol. Chem. 272*, 10853−10858.
8. Bode, W., Engh, R., Musil, D., Thiele, U., Huber, R., Karshikov, A., Brzin, J., Kos, J., and Turk, V. (1988) *EMBO J. 7*, 2593−2599.
9. Ekiel, I., Abrahamson, M., Fulton, D. B., Lindahl, P., Storer, A. C., Levadoux, W., Lafrance, M., Labelle, S., Pomerleau, Y., Groleau, D., LeSauteur, L., and Gehring, K. (1997) *J. Mol. Biol. 271*, 266−277.
10. Hall, A., Dalbøge, H., Grubb, A., and Abrahamson, M. (1993) *Biochem. J. 291*, 123−129.
11. Björk, I., Brieditis, I., and Abrahamson, M. (1995) *Biochem. J. 306*, 513−518.
12. Freije, J. P., Abrahamson, M., Olafsson, I., Velasco, G., Grubb, A., and López-Otín, C. (1991) *J. Biol. Chem. 266*, 20538−20543.
13. Grubb, A., Löfberg, H., and Barrett, A. J. (1984) *FEBS Lett. 170*, 370−374.
14. Hall, A., Håkansson, K., Mason, R., Grubb, A., and Abrahamson, M. (1995) *J. Biol. Chem. 270*, 5115−5121.
15. Xin, X.-Q., Gunesekera, B., and Mason, R. (1992) *Arch. Biochem. Biophys. 299*, 334−339.
16. Abrahamson, M., Dalbøge, H., Olafsson, I., Carlsen, S., and Grubb, A. (1988) *FEBS Lett. 236*, 14−18.
17. Sambrook, J., Fritsch, E. F., and Maniatis, T. (1989) *Molecular cloning: a laboratory manual*, 2nd ed., Cold Spring Harbor Laboratory Press, Cold Spring Harbor, NY.
18. Dalbøge, H., Bech Jensen, E., Tøttrup, H., Grubb, A., Abrahamson, M., Olafsson, I., and Carlsen, S. (1989) *Gene 79*, 325−332.
19. Schägger, H., and von Jagow, G. (1987) *Anal. Biochem. 166*, 368−379.
20. Olafsson, I., Gudmundsson, G., Abrahamson, M., Jensson, O., and Grubb, A. (1990) *Scand. J. Clin. Lab. Invest. 50*, 85−93.
21. Grubb, A., Abrahamson, M., Olafsson, I., Trojnar, J., Kasprzykowska, R., Kasprzykowski, F., and Grzonka, Z. (1990) *Biol. Chem. Hoppe-Seyler 371* (Suppl.), 137−144.
22. Henderson, P. J. F. (1972) *Biochem. J. 127*, 321−333.
23. Barrett, A. J., and Kirschke, H. (1981) *Methods Enzymol. 80*, 535−561.
24. Weiner, S. J., Kollman, P. A., Nguyen, D. T., and Case, D. A. (1986) *J. Comput. Chem. 7*, 230−252.
25. Weiner, S. J., Kollman, P. A., Case, D. A., Singh, U. C., Ghio, C., Algona, G., Profeta, S., Jr., and Weiner, P. (1984) *J. Am. Chem. Soc. 106*, 765−784.
26. Abrahamson, M., Ritonja, A., Brown, M., Grubb, A., Machleidt, W., and Barrett, A. J. (1987) *J. Biol. Chem. 262*, 9688−9694.
27. Buttle, D., Ritonja, A., Dando, P., Abrahamson, M., Shaw, E., Wikström, P., Turk, V., and Barrett, A. J. (1990) *FEBS Lett. 262*, 58−60.
28. Dieckmann, T., Mitschang, L., Hofmann, M., Kos, J., Turk, V., Auerswald, E. A., Jaenicke, R., and Oschkinat, H. (1993) *J. Mol. Biol. 234*, 1084−1059.
29. Abrahamson, M., and Grubb, A. (1994) *Proc. Natl. Acad. Sci. U.S.A. 91*, 1416−1420.
30. Ekiel, I., and Abrahamson, M. (1996) *J. Biol. Chem. 271*, 1314−1321.
31. Machleidt, W., Thiele, U., Laber, B., Assfalg-Machleidt, I., Esterl, A., Wiegand, G., Kos, J., Turk, V., and Bode, W. (1989) *FEBS Lett. 243*, 234−238.
32. Lindahl, P., Abrahamson, M., and Björk, I. (1992) *Biochem. J. 281*, 49−55.
33. Martin, J. R., Craven, C. J., Jerala, R., Kroon-Zitko, L., Zerovnik, E., Turk, V., and Waltho, J. P. (1995) *J. Mol. Biol. 246*, 331−343.
34. Stubbs, M. T., Laber, B., Bode, W., Huber, R., Jerala, R., Lenarcic, B., and Turk, V. (1990) *EMBO J. 9*, 1939−1947.
35. Illy, C., Quraishi, O., Wang, J., Purisima, E., Vernet, T., and Mort, J. S. (1997) *J. Biol. Chem. 272*, 1197−1202.
36. Björk, I., Pol, E., Raub-Segall, E., Abrahamson, M., Rowan, A., and Mort, J. S. (1994) *Biochem. J. 299*, 219−225.
37. Björk, I., Brieditis, I., Raub-Segall, E., Pol, E., Håkansson, K., and Abrahamson, M. (1996) *Biochemistry 35*, 10720−10726.
38. Lindahl, P., Ripoll, D., Abrahamson, M., Mort, J. M., and Storer, A. C. (1994) *Biochemistry 33*, 4384−4392.
39. Auerswald, E. A., Genenger, G., Assfalg-Machleidt, I., Machleidt, W., Engh, R. A., and Fritz, H. (1992) *Eur. J. Biochem. 209*, 837−845.

BI971197J